Title

The initial appraisal of buried DAS system in CO2CRC Otway Project: the comparison of buried standard fibre-optic and helically wound cables using 2D imaging

Journal

Exploration Geophysics, 50(1)

ISSN

0812-3985

Authors

Yavuz, Sinem
Freifeld, Barry
Pevzner, Roman
et al.

Publication Date

2019-01-02

DOI

10.1080/08123985.2018.1561147

Peer reviewed

The initial appraisal of buried DAS system in CO2CRC Otway Project: the comparison of buried standard fibre-optic and helically wound cables using 2D imaging

Sinem Yavuz [a,b], Barry Freifeld[c], Roman Pevzner[a,b], Aleksandar Dzunic[a,b], Sasha Ziramov[a,b], Andrej Bóna[a,b], Julia Correa[a,b], Konstantin Tertyshnikov[a,b], Milovan Urosevic[a,b], Michelle Robertson[c] and Thomas Daley[c]

[a]Exploration Geophysics, WA School of Mines: Minerals, Energy and Chemical Engineering, Curtin University, Perth, Western Australia, Australia; [b]CO2CRC, Carlton, Victoria, Australia; [c] Lawrence Berkeley National Laboratory, Berkeley, CA, USA

ABSTRACT

This study aims to assess the ability of shallow distributed acoustic sensing (DAS) to serve as a cost-effective seismic sensor array for permanent monitoring applications. To this end, as part of the CO2CRC seismic monitoring program, a fibre-optic DAS array was deployed alongside a permanently buried geophone array at the Otway Project site (Victoria, Australia). The DAS array consisted of a standard commercially available tactical fibre-optic cable, which was deployed in 0.8 m deep trenches. A custom-designed helically wound (HW) cable was also deployed in one of the DAS trenches for comparison of the cable designs. Simultaneous acquisition of the seismic data was carried out using ~ 3000 vibroseis source points and geophones, DAS standard and HW cables. For initial assessment of the seismic images acquired with DAS and to compare different cable designs, preliminary 2D seismic reflection processing is conducted on both DAS cables and geophone data along a single 2D line. The geophone data processing guided processing of the DAS data. Several shallow structures (100–450 ms) and some important reflectors at 450–600 ms are observed on the final DAS images. Comparison of the two different DAS cable types demonstrated that seismic imaging would benefit DAS technology. However, the benefit of utilising HW cable is modest compared with the standard cable. The workflows and results of this study pave the way for processing of the 3D seismic data set acquired with the DAS array, as well as further detailed analysis of the DAS cables and the system itself.

KEYWORDS: distributed acoustic sensor, helically wound cable, seismic monitoring

Introduction

Time-lapse (TL) seismic has great potential for monitoring fluid injection and possible leakage in global carbon geosequestration projects (White 2011; Jenkins et al. 2012). The success of TL seismic for CO_2 surveillance depends on overcoming a number of challenges, such as prolonged periods between the baseline and monitor surveys, the possible environmental impact of seismic acquisition and the relatively poor repeatability of land surveys.

These challenges can have a significant impact on the effectiveness and cost of conventional TL 3D seismic (otherwise known as 4D seismic). One method to reduce the cost and increase the number of surveys is to utilise permanent seismic receiver arrays.

One promising type of permanent seismic sensor is the distributed acoustic sensor, which works by emitting a series of laser pulses to an optical fibre. A small amount of the light is backscattered by small-scale heterogeneities in the fibre and returns to the interrogation unit. The interrogation unit in a DAS system processes the backscattered light for every pulse to profile strain changes within the optical fibre structure. An acoustic field can be measured along the whole fibre by recording the returning signal against time. Advances in optical interferometric methods allow this technology to use commercial telecommunication optical fibres. DAS has shown numerous field applications over the past decade in seismic surveys (Hornman et al. 2013; Mateeva et al. 2014; Parker, Shatalin, and Farhadiroushan 2014; Correa et al. 2017a, 2017b; Hornman 2017). The theory behind DAS technology is discussed thoroughly in Parker, Shatalin, and Farhadiroushan (2014), Kuvshinov (2016) and Hartog (2017). Key advantages of DAS compared with geophones include relatively low cost, easy deployment, the relatively long lifetime of the fibre-optic cables, and very high spatial coverage (tens of kilometres of continuous fibre cables). These features could potentially lead to significant improvements in the cost-effectiveness of TL seismic monitoring.

Stage 2C of the CO2CRC Otway Project is focused on conducting a comprehensive seismic monitoring programme using various seismic techniques, data analysis, and modelling to detect and monitor the evolution of a small (15 kilo-tonnes) supercritical CO_2/CH_4 plume injected into a saline aquifer located at 1500 m depth. The biggest challenge for this experiment is the high ambient noise level compared with the strength of the TL signal (Pevzner et al. 2013, 2017). One option to reduce the noise level is to use buried geophones. To explore this possibility, a small set of permanent receivers was tested at various depths in 2012 and provided drastically improved results in the repeatability of TL seismic (Shulakova et al. 2015). This experiment became the benchmark for future experimental designs. Concurrent with this test, Daley et al. (2013) tested DAS acquisition and obtained promising results. These tests were followed in 2015 by installation of a permanent 3D receiver array, a permanent 3D DAS array and a retrievable borehole geophone array in the monitoring well, as well as a DAS array in the injection well (Correa et al. 2018). The purpose of these installations was to perform numerous experiments to ascertain the optimal TL seismic approach for monitoring the emplaced CO_2 plume. The iDAS system (Silixa Ltd, Elstree, UK), including a 3D buried telecommunication-style fibre-optic cable array, was used to test the feasibility of DAS technology for TL seismic. A prototype helically wound (HW) cable (Kuvshinov 2016) was also deployed along with standard cables to allow the comparison of two different DAS cable designs for the optimisation of DAS technology.

Collocating the DAS system with conventional geophones gives a rare opportunity to assess its performance quantitatively. Following installation, conventional vibroseis baseline 3D surface seismic data were acquired using buried geophones, a 3D standard DAS array and a 2D HW cable. To set a benchmark for 3D DAS processing and imaging, we selected a 2D line of geophones and both DAS data sets located in the same trench. Yavuz et al. (2016) presented the results of the pilot DAS surface seismic data analysis and the subsurface images processed using the conventional data acquired with the geophone array as a guide. In this study, to optimise the DAS data processing, we perform a direct comparison of standard fibre-optic and HW cables through to seismic imaging. The HW cable was produced specifically to avoid the issue of directionality in the DAS data, because the signal decays as cosine squared of the angles of incidence in DAS data, in contrast to geophones with which the signal decays as cosine of the angles of incidence. Because of the strong ground roll on the DAS data, the signal levels visually not pronounced for deep reflections, which are present on geophone sections. Hence, in this study, we focus on developing a processing workflow for imaging a few known near-surface reflections (up to 600 ms). The results of this 2D study can form a basis for the development of the workflow for 3D DAS data processing and analysis.

Field set-up

The Stage 2C experiment involved the deployment of a permanent geophone array, fibre-optic DAS system, and related infrastructure and equipment. Quality control (QC) was then conducted on the systems followed by the simultaneous acquisition of 3D seismic data for monitoring the CO_2 plume during the injection tests (Figure 1). The Otway site permanent seismic array consists of 11 receiver lines (Figure 2) with 908 high-sensitivity SG-5 vertical geophones capable of recording data down to 5 Hz. These geophones were buried 4 m deep in polyvinyl chloride (PVC)-cased bores with a receiver spacing of 15 m. Geophone installation depth was derived after the series of tests conducted in 2012 (Shulakova et al. 2015). As a part of these tests, we deployed an array of surface and buried geophones (at different depths) onsite and acquired single cross-spread survey. No evidence of higher attenuation at the near surface was noticed. However, burying the geophones deeper than 3 m drastically reduced the wind noise. The same conclusion could be reached from a direct comparison of the surface and buried geophones carried out for the main array and presented in Pevzner et al. (2015). It was also an expectation that 4 m depth would ensure that the geophones were deployed below the water table. Each receiver line of the buried system extends from 890 m to 1460 m with a receiver line spacing of 100 m. After deployment of the permanent geophone array, a DAS fibre-optic system including standard fibre-optic and HW cables was also deployed. Because we were also aiming to bury cables for the geophone system, to avoid having anything left on the surface (to reduce the invasiveness of the survey), we used 0.8 m deep trenches for this. The depth of the trench was selected such that the cables would not be damaged by ploughing. The standard telecom fibre cable has slight helical winding of the loose fibre tube at an angle of ~ 11° from the axial centre of the cable, consistent with a telecommunications cable style construction. The slight winding of 11° allows for the DAS receiver spacing to be almost 1 m of fibre per 1 m of cable. The HW cable has a steeper fibre winding of 30° from the axial centre. A standard fibre-optic cable was deployed in 80 cm deep trenches along the 11 geophone receiver lines (Figure 1). We used the standard loose tube telecom cable design for the burial. Most of these cables have tubes with fibres wound around the strength member to protect the fibre from excessive stretch while being deployed. Our DAS acquisitions were made with a single mode fibre. The HW cable was experimental and multiple buffer tubes with fibres were installed to keep the structure round because the manufacturer did not have solid plastic rods available. Subsequent constructions reduced the number of fibre tubes to two. For direct comparison of the fibre responses between the two cable types, the HW cable was deployed in the same trench as the geophone receiver line 5. Both standard and HW cables were installed in a “U” configuration to acquire data in both south-to-north and north-to-south directions. The “U” configuration eliminates the need for end splices in the trenches, reducing potential signal degradation at the expense of increased data volume. The Otway experimental site has a DAS array with a total length exceeding 36 km, including the DAS cables installed in the boreholes.

Figure 1. Experimental set-up. (a) Trencher digging the trench, (b) boring for the 4 m deep PVC-cased bores to install geophones, (c) installation of a geophone in a bore and the geophone cables, (d) blue iDAS fibre-optic cables laying at the bottom of each trench, and (e) HW cable buried in the line 5 trench for direct comparison (after Hornman et al. 2013).

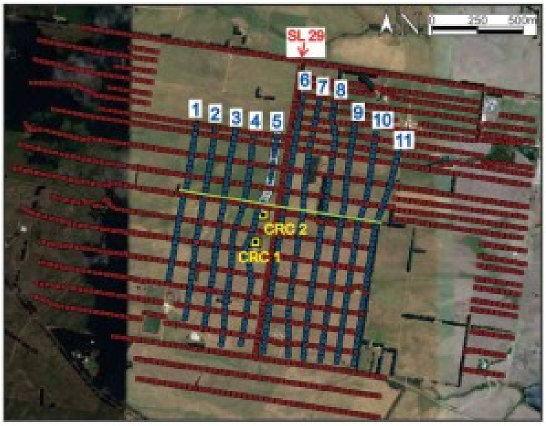

Figure 2. Map view of the Otway site for the CO2CRC Stage 2C seismic survey, March 2015. Eleven lines of surface geophones and baseline survey vibroseis source points are shown as blue and red dots, respectively. The standard fibre-optic DAS cable is collocated along the 11 geophone receiver lines, and the HW cable is only buried in line 5, as highlighted by the white dots. CRC-1 and CRC-2 wells and the backbone trench (green) are also highlighted (modified from Yavuz et al., 2016).

CRC-2 well is the injector well for Stage 2C of the Otway Project containing a fibre-optic cable attached to tubing. CRC-2 has a depth of ~ 1.5 km, 300 m less than CRC-1 well, which for the Stage 2C experiment serves as a monitoring well. Both CRC-1 and CRC-2 are vertical wells located 150 m apart. The seismic recording facility (Seismic Lab) is located near the CRC-2 well head. Twenty-two fibre cables along the receiver lines and the backbone cables are fed along the backbone trench. These cables extend the control boxes through to the Seismic Lab. Figure 2 shows the map view of the Otway site for the March 2015 deployments.

To make processing and visualisation of the data more efficient, the DAS array is split into two manageable lengths on two separate iDAS data acquisition set-ups. Unit iDAS-1 recorded acoustic data from the CRC-2 wellbore fibre loop and the standard fibre loops in lines 4, 5, 6 and 7. Unit iDAS-2 recorded acoustic data from fibre loops from receiver lines 1, 2, 3, 8, 9, 10 and 11. The standard single mode fibres used in the acquisition are designed for the laser wavelengths of 1300–1500 nm. Pulse width of the laser was 50 ns. The intensity of the laser was changed a couple of times during the survey because we were aiming to select the best laser intensity. The maximum pulse frequency for this survey is ~ 5 kHz. However, a smaller pulse repetition frequency of ~ 2 kHz was selected. To locate the recording channels along the DAS cable during the seismic survey, we conducted a series of tap tests. During these tests, DAS data were recorded while having a seismic source (usually just a sledgehammer) activated at a known location above the buried fibre-optic cables. Thus, the position of the seismic source along the cable, as seen on the record, is related back to the surface coordinate and receiver station number. After the tap tests and final QC on the systems, simultaneous 3D seismic data acquisition was conducted on the geophone array and the DAS system using 3003 vibroseis source points. There are two large areas to which we did not have access during this survey. To account for missing shots in these areas, a narrower source line spacing was chosen next to these areas to increase the fold. Two 26000 lb INOVA Vibrators were utilised with a single 24-s sweep set to a frequency range of 6–150 Hz and 0.5 s taper. The data were recorded with 5 s listening time and 1 ms sampling rate. The receiver spacing of both fibre-optic cables is 1 m so that a total of 26 804 channels of data were recorded, with a total data volume of 13.5 TB.

Fast-track pilot processing

The main objective of this study is to perform an overall assessment of the DAS data to optimise the data processing of the large 3D DAS data set (Correa et al. 2017a). To this end, we perform preliminary 2D data processing of both geophone and DAS data sets along a single 2D line. Figure 2 shows the selected receiver line 5 consisting of 80 channels with 15 m receiver spacing and almost in parallel with selected shot line 29 consisting of 107 shots with a shot spacing of 15 m. As mentioned previously, looped DAS fibre cables allowed us to acquire the data in two parallel segments. However, for simplicity, we process only one side of each cable. Both the standard fibre-optic cable with 1176 channels and the HW cable with 760 channels have ~ 1 m receiver spacing. This spatial sampling was preselected in the iDAS unit prior to acquisition, as was the gauge length. Because the cables are connected to each other, the same spatial sampling applies to both. It should be noted that, unlike single geophone sensors, DAS channels are formed by a finite length (gauge) of fibre-optic cable with temporal variation in scattering from the opposite side of this length. This is used to estimate the acoustic signal by measuring the difference in phase between two positions separated by a distance called the gauge length (Bona et al. 2017). The gauge length employed in this experiment was 10 m, and the measurement was assigned to the centre of the gauge.

First, because receiver line 5 had a 2D crooked-line profile, to improve signal alignment before CMP stacking, a crooked line geometry is applied to both geophone and DAS data sets as displayed in Figure 3. A bin size of 10 m is utilised to account for the gauge length of the DAS data and improve the alignment of reflections. Figure 3 also shows the CMP fold maps of all data sets. The CMP fold of DAS data is high relative to the geophone data, which is to be expected considering the reduced receiver (sensing) spacing. After the geometry set-up, we analyse all raw data sets in terms of acoustic events. A shot location closer to the middle of the shot line is marked with a green star in Figure 3 and used as the reference shot gather in Figure 4. The geophone data raw shot gather (Figure 4a) shows clear direct arrivals and a few shallow reflections are prominent and continuous. On the DAS raw shot records (Figure 4b,c), direct arrivals are visible, but the reflections are not apparent. Furthermore, all the data sets show strong ground roll. The ambient noise level and ground roll intensity are higher in DAS compared with geophone data as observed on the reflection strength section of the same shot gathers in Figure 5. Strong surface waves in the DAS data suggest that their dispersion can be used for characterisation of near-surface properties (Park, Miller, and Xia 1999).

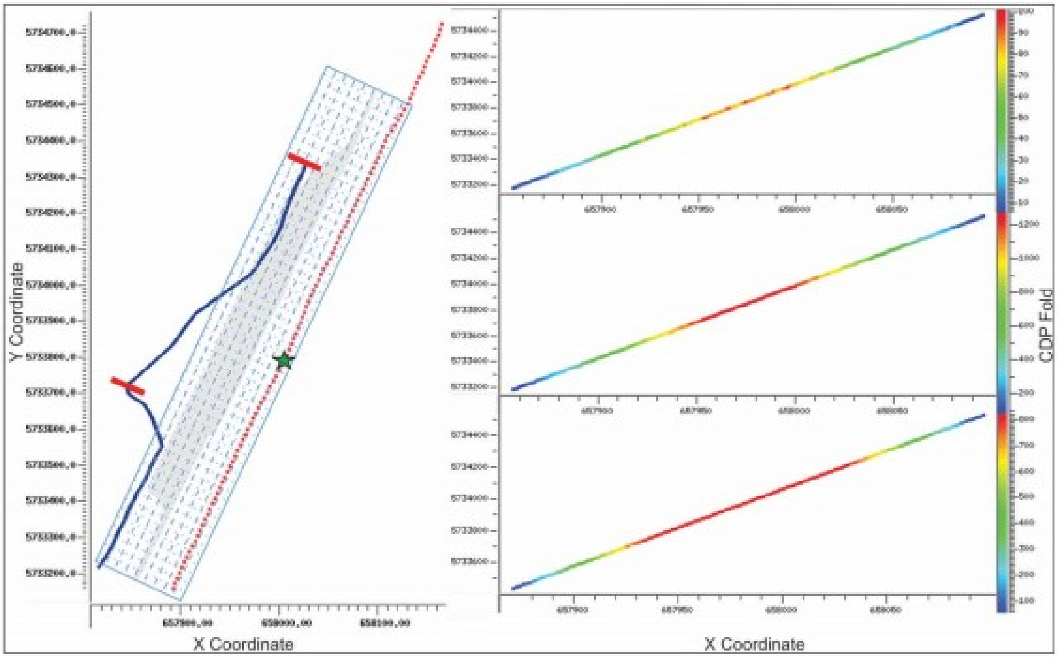

Figure 3. Crooked line binning of both standard fibre-optic DAS and geophone data sets. Red stars and blue crosses show the shot points, and standard fibre-optic DAS cable and geophones, respectively. Standard fibre-optic DAS and geophone data are binned in green cells and are superimposed on the midpoints. Red lines indicate the start and end of the HW cable laid in the same trench as the standard fibre-optic DAS. The shot point displayed in Figure 4 is highlighted with a star. CDP fold maps of the geophone, standard cable and HW cable data sets are displayed on the right from top to bottom.

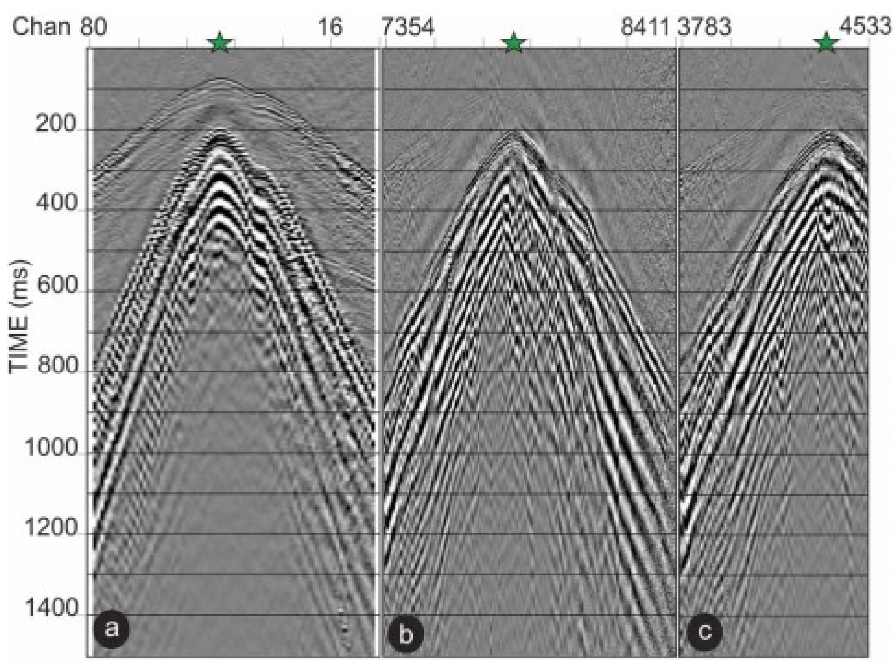

Figure 4. A raw shot gather (see Figure 3 for the location) of (a) geophone, (b) standard fibre-optic and (c) HW cable DAS data. The shot point is indicated by a star.

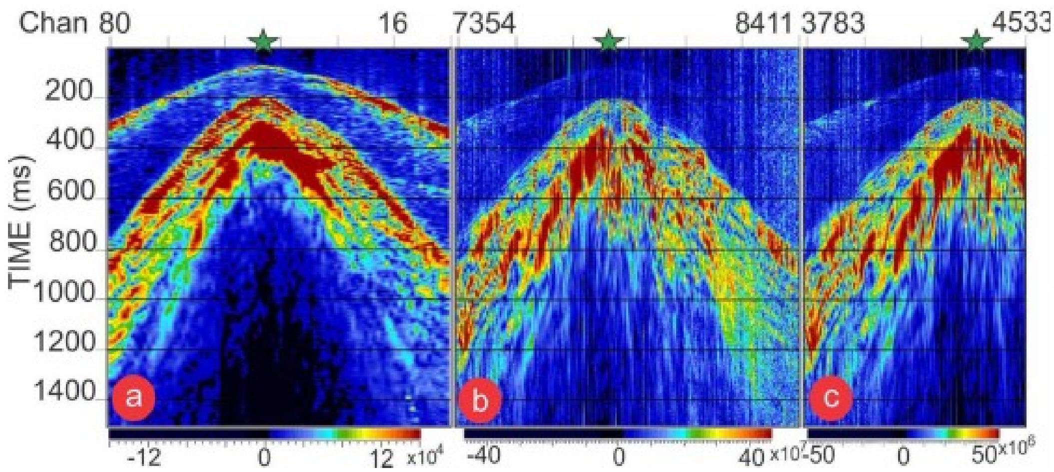

Figure 5. Reflection strength of the raw shot gathers (see Figure 3 for the location) of (a) geophone, (b) standard fibre-optic and (c) HW cable DAS data. The shot point is indicated by a star.

After thorough QC of the data sets, we produce quick brute stacks for all data sets with a simple processing flow (Figure 6). This processing flow includes the application of top and bottom mutes to preserve the data in a window between the direct wave and ground roll, an automatic gain control (AGC) (1 s) and bandpass filter (1–25–50–90 Hz). The two strong reflections located between 450 and 600 ms are imaged on the brute stack of the geophone data (Figure 6a). Hence, we then try to stack the DAS data sets in a similar way for direct comparison. Equivalent reflections are visible on both the geophone and DAS brute stacks (Figure 6b,c).

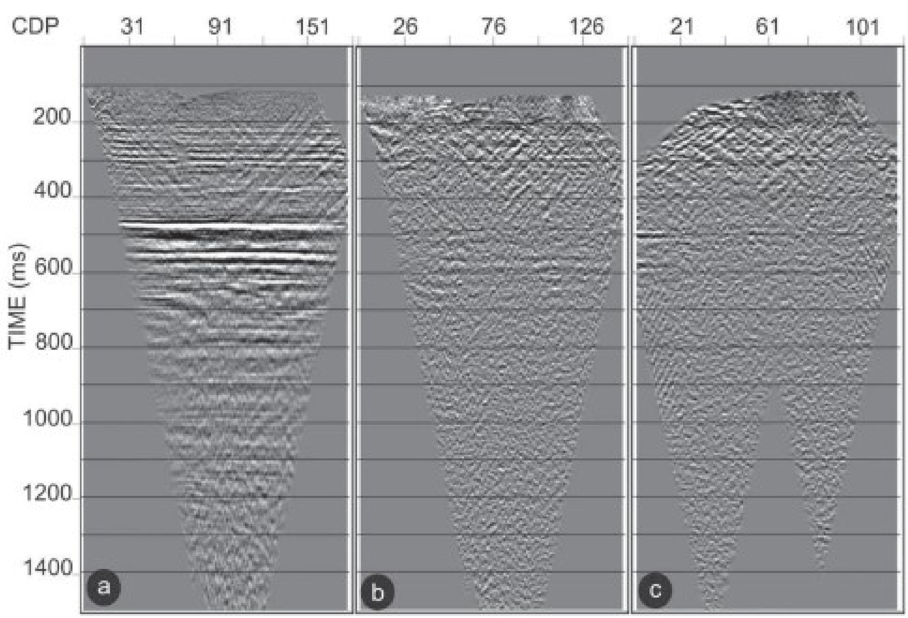

Figure 6. Brute stack sections of (a) geophone, (b) standard fibre-optic DAS and (c) HW cable DAS data with a ground roll and direct wave mute.

Geophone data processing

To evaluate the DAS data for seismic monitoring surveys and the direct comparison of the two different cable designs, the seismic data processing is further refined. To this end, we first build a processing flow for the geophone data and utilise it to assist the DAS data processing. The processing flow for the geophone data is outlined in Table 1. The first key processing step for the geophone data is an assessment of several filters to eliminate surface waves and ambient noise. Among all tested filter options, the linear Radon filter provides the best results by suppressing the noise associated with ground roll. We apply this filter in a window specifically designed to encompass only the ground roll to avoid any undesired distortion on the shallow reflections. Figure 7 shows gathers before and after Radon filter. The results suggest that Radon filter successfully attenuates the ground roll.

Table 1. Geophone data processing flow.

1.	Geometry specification / binning (10 m)
2.	Burst noise removal
3.	Trace correlation
4.	Interactive radon / τ–p analysis
5.	Trace shift 500 ms down
6.	Window processing (defining a window for Radon filter application)
7.	Application of automatic gain control (AGC) using data window
8.	Radon filter: linear, number of p-values 500, p-value interest 500–3500 ms, white noise 0.03%
9.	AGC removal
10.	Trace shift 500 ms down
11.	Interactive velocity analysis (iterative): using the common depth point (CVS)-derived velocities as a guide function: on CDP supergathers created with five in-lines and cross-lines for every tenth in-line and cross-line
11.	Normal moveout (NMO) corrections – stretch mute 55
13.	Bandpass filter: 2–30–90–140 Hz Ormsby
14.	2D spatial filter (simple alpha-trimmed mean)
15.	AGC (500 ms, centred)
16.	Stack
17.	Spectral shaping (1–25–60–90)

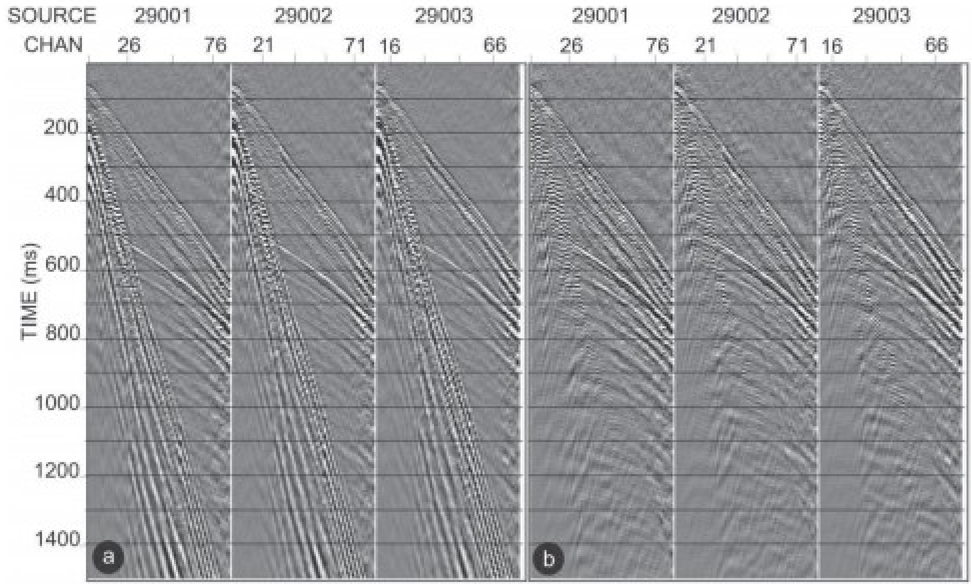

Figure 7. Geophone data shot gathers (a) before and (b) after removal of the ground roll with a linear Radon filter.

The next step in the geophone data processing is the interactive velocity analysis. The guide function for interactive velocity analysis on geophone data is extracted from the known velocity field, which was mapped in previous seismic surveys at the Otway site (Shulakova et al. 2015). We also perform an interactive frequency spectrum analysis. This demonstrates that the frequency range of the geophone data is between 30 and 90 Hz. We then design our bandpass filter accordingly. After application of this filter, to further suppress ambient noise, we apply a simple alpha-trimmed mean filter, which enhances the continuity of horizontal events. Finally, to increase the temporal resolution, spectral shaping within the frequency range 1–25–60–90 Hz is applied. Comparison of the final stacked section of geophone data (Figure 8a) with its initial brute stack (Figure 6a) shows that refined data processing can recover signal up to 800 ms. The shallow reflections around 100–450 ms and two other strong reflections located between 450 and 600 ms are imaged (Figure 8a). However, deeper reflections are severely affected by surface waves and ambient noise.

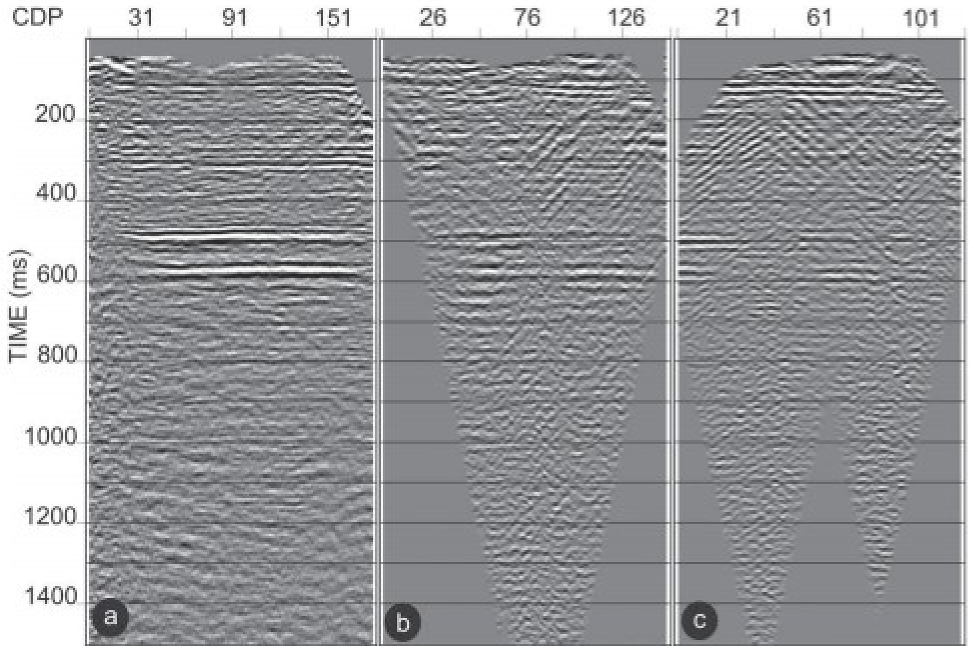

Figure 8. Final stack sections of (a) geophone, (b) standard fibre-optic DAS and (c) HW cable DAS data.

DAS data processing

After the geophone data processing, we focus on the DAS data processing. Both data sets (standard fibre-optic and the HW cables) have similar processing streams applied. The full processing flow for both DAS data sets is outlined in Table 2. The raw DAS data QC indicate that ground roll is the dominant noise in the data (Figures 4 and 5), and ground roll attenuation would be the most critical component for signal-to-noise ratio (SNR) improvement. In the DAS processing, we perform several key trials specifically designed to reduce the effect of the strong surface waves. These trials are guided by the geophone data processing. Hence, we assess all possible filter types such as fan filter, F–K filter and Radon filter for ground roll removal. However, because the linear Radon filter delivered a good outcome for the geophone data processing, we utilise it in the DAS data processing as well. Similar to geophone data processing, the Radon filter is interactively parameterised for both data sets and applied in a window to preserve the signal. After the removal of ground roll, we observe residual noise of parabolic shape. This event is identified as reflected P–S-converted waves as seen on a standard DAS data shot section (Figure 9). To suppress the converted waves, we interactively test a parabolic Radon filter application. Despite these efforts, the results are still far from satisfactory. Consequently, we decide to proceed with a bottom mute to surgically remove the surface waves from stacking.

Table 2. Das data processing flow.

1.	Geometry specification / binning (10 m)
2.	Burst noise removal
3.	Trace correlation
4.	Trace mute (bottom mute for ground roll and below)
5.	2D spatial filter (2D convolutional filter)
6.	Normal moveout (NMO) corrections with a single velocity function
7.	Bandpass filter: 15–30–60–120 Hz Ormsby
8.	2D spatial filter (simple alpha-trimmed mean)
9.	Automatic gain control (AGC; 500 ms, centred)
10.	Stack
11.	FX deconvolution

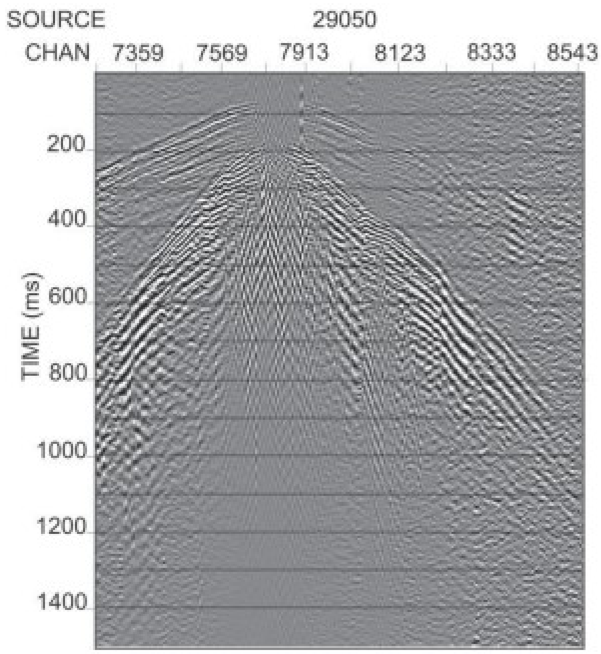

Figure 9. DAS data shot section after application of a 2D convolutional filter for airwave removal.

The noise associated with the airwave is suppressed with the application of a 2D convolutional filter, followed by a simple alpha-trimmed mean filter to suppress ambient noise. Interactive velocity analysis is then performed for both DAS data sets using a guide function based on the velocity field obtained from geophone data processing. However, in the DAS data processing, a single velocity function provides the best result and is used in the NMO application. A bandpass filter (5–30–60–120 Hz) followed by an FX deconvolution is applied to the stacked data. Figure 8(b,c) shows the final stack sections of DAS data sets. The two strong reflections around 450–600 ms, as well as a few shallower reflections, are visible in the final DAS stacked sections.

To evaluate the performance of HW *versus* a standard telecommunication-style cable, it is desirable to provide a direct comparison between the two data sets with surveys that have the same fold. To this end, the standard fibre-optic cable is limited to the HW cable length and binned using the same crooked line geometry as in the HW cable. Raw shot gather analysis shows that the HW cable provides slightly better images than the standard fibre-optic cable. However, because both cables were buried under unsaturated and unconsolidated backfill, some shot gathers show inconsistent results. The brute stacks, which were previously produced in the pilot processing for all data sets, are also created for the limited standard DAS data. Figure 10 displays the muted brute stack of the limited standard fibre-optic DAS cable (Figure 10a) and the muted brute stack of HW cable data (Figure 10b). After application of the same processing flow (Table 2) to the limited standard fibre-optic cable data, the resulting section is compared with the final HW cable data stack section in Figure 11. It is clear that the HW cable data section has significantly better resolution for the reflection at 100–150 ms (Figure 11b). The noise created by the ground roll and surface waves appears to be less pervasive on the HW cable image compared with the standard DAS image. However, the deeper reflections around 450–600 ms are better imaged on the standard fibre-optic cable image (Figure 11a).

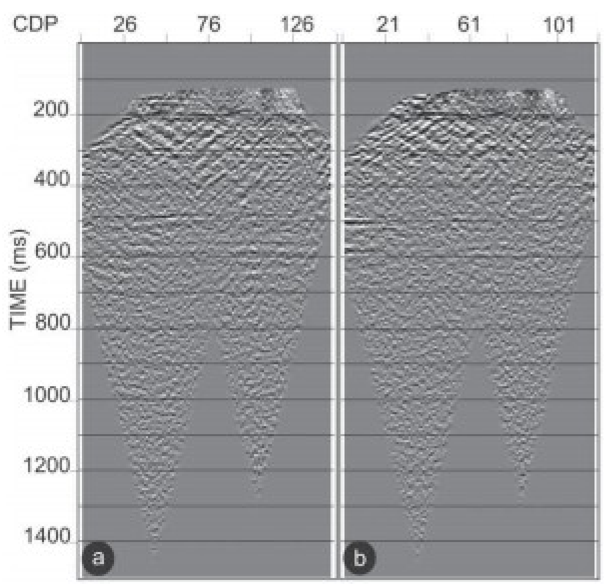

Figure 10. Brute stack sections of (a) limited standard fibre-optic and (b) HW cable DAS data.

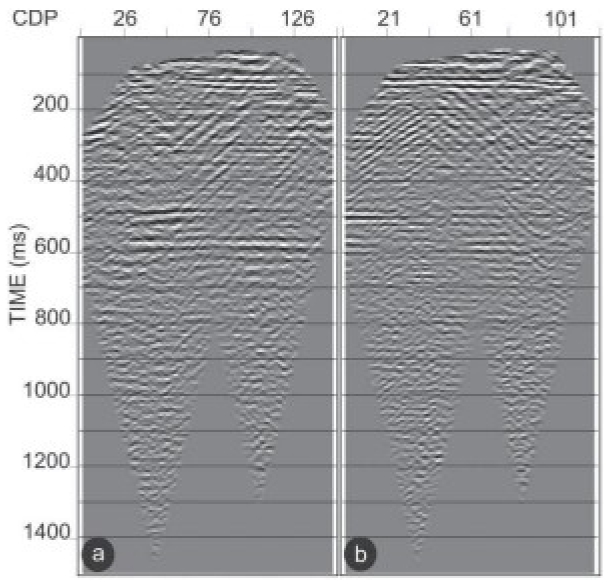

Figure 11. Final stack sections of (a) limited standard fibre-optic and (b) HW cable DAS data.

Discussion and conclusions

The Otway Stage 2C experiment provided an excellent opportunity to test the effectiveness of different forms of seismic acquisition hardware for TL seismic. DAS is a relatively new but extremely promising technology that can potentially provide a cost- and time-effective solution in surface and borehole seismic monitoring. A surface seismic monitoring system utilising a permanent 3D geophone array was acquired in conjunction with a 3D DAS array. To investigate the performance of DAS compared with a collocated geophone array, we selected a 2D subset comprised of one receiver line instrumented with both standard fibre-optic and an HW cables to record into using a parallel source line. Seismic data processing was employed for the initial assessment DAS data sets as well as the direct comparison of the different cable designs.

DAS measures changes in relative strain along the cable. Hence, in a surface seismic survey design like ours, it is sensitive to seismic events that travel in the horizontal direction, such as ground roll. The changes that occur in the vertical direction caused by events such as reflections arrive perpendicular to the fibre and therefore fall within its almost blind component. This broadside sensitivity issue is obvious on the brute stacked seismic sections. Compared with the strong and continuous direct arrivals and reflections from the geophone data, the raw DAS data set provided visible direct arrivals and no apparent reflections, most likely due to the ambient noise level and strong ground roll and surface wave intensity. A data processing flow is created for both DAS data sets using the geophone data processing as a guide. The main challenge in the processing is to suppress ground roll and surface waves in all data sets. Although a linear Radon filter has given good results on geophone data, the DAS data sets had to be simply muted to remove this coherent noise due to a low SNR and broadside sensitivity issue. DAS data were still capable of imaging the known reflections. Better continuity of the shallow reflector around 100–150 ms is observed on the HW cable data compared with the standard fibre-optic cable and geophone data (Figure 8). However, deeper reflections are better imaged in the standard fibre-optic seismic section. Direct comparison of DAS cables for improved imaging of the reflectors around 100–150 ms on Figure 11 shows better resolution and a higher SNR for HW compared with standard cable. This is probably because the helical winding increases the broadside sensitivity of the DAS cable. However, the shallow reflectors (0–100 ms) on all the data sets look very different. These differences are probably caused by the effect of differences in the elastic properties of, or their coupling to, the unsaturated and unconsolidated backfill at the specific locations of the two DAS cables. Despite the fact that DAS has low SNR, the known reflectors around 450–600 ms are still recovered on both HW cable and standard fibre. The subsequent analyses and 3D data processing of the DAS data highly benefited from the insights achieved from this study (Bona et al. 2017; Correa et al. 2017a, 2017b).

Acknowledgements

The CO2CRC Otway Stage 2C Project received funding through CO2CRC's industry members and research partners, the Australian Government, the Victorian State Government and the Global CCS Institute. The authors wish to acknowledge financial assistance provided through Australian National Low Emissions Coal Research and Development (ANLEC R&D) supported by the Australian Coal Association Low Emissions Technology Limited and the Australian Government through the Clean Energy Initiative. Funding for LBNL was provided through the Carbon Storage Program, U.S. DOE, Assistant Secretary for Fossil Energy, Office of Clean Coal and Carbon Management through the NETL. We acknowledge the help of M. Hehir and D. Popik (Curtin University), T. Roberts (Westlog), I. McLintock and P. Dumesny (Upstream Production Solutions) in conducting the field surveys.

References

Bona, A., T. Dean, J. Correa, R. Pevzner, K. Tertyshnikov, and L. Van Zaanen. 2017. Amplitude and phase response of DAS receivers. 79th Conference and Exhibition, EAGE, Extended Abstracts, doi:10.3997/2214-4609.201701200.

Correa, J., A. Egorov, K. Tertyshnikov, A. Bona, R. Pevzner, T. Dean, B. Freifeld, and S. Marshall. 2017b. Analysis of signal to noise and directivity characteristics of DAS VSP at near and far offsets — A CO2CRC Otway Project data example. *The Leading Edge* 36, no. 12: 994a1–a7. doi: 10.1190/tle36120994a1.1

Correa, J., B. Freifeld, M. Robertson, R. Pevzner, A. Bona, D. Popik, S. Yavuz, et al. 2017a. Distributed acoustic sensing applied to 4D seismic: preliminary results from the CO2CRC Otway site field trials. 79th EAGE Conference & Exhibition 2017, Paris, France, Tu A1 15.

Correa, J., P. Pevzner, A. Bona, K. Tertyshnikov, B. Freifeld, M. Robertson, and T. Daley. 2018. 3D VSP acquired with das on tubing installation: a case study from the CO2CRC Otway Project. *Interpretation*. doi:10.1190/int-2018-0086.1.

Daley, T. M., B. M. Freifeld, J. Ajo-Franklin, S. Dou, R. Pevzner, V. Shulakova, S. Kashikar, et al. 2013. Field testing of fiber-optic distributed acoustic sensing (DAS) for subsurface seismic monitoring. *The Leading Edge* 32, no. 6: 699–706. doi: 10.1190/tle32060699.1

Hartog, A. 2017. *An introduction to distributed optical fibre sensors, series in fiber optic sensors*. FL, USA: CRC Press Taylor & Francis Group. ISBN 9781138082694.

Hornman, J. C. 2017. Field trial of seismic recording using distributed acoustic sensing with broadside sensitive fibre-optic cables. *Geophysical Prospecting* 65: 35–46. doi:10.1111/1365-2478.12358.

Hornman, K., B. Kuvshinov, P. Zwartjes, and A. Franzen. 2013. Field trial of a broad-side sensitive distributed acoustic sensing cable for surface seismic. In Proceedings of the 75th EAGE Conference & Exhibition, London, UK, June 2013.

Jenkins, C. R., P. J. Cook, J. Ennis-King, J. Undershultz, C. Boreham, T. Dance, P. de Caritat, et al. 2012. Safe storage and effective monitoring of CO2 in depleted gas fields. *Proceedings of the National Academy of Sciences* 109: E35–41. doi: 10.1073/pnas.1107255108

Kuvshinov, B. N. 2016. Interaction of helically wound fibre-optic cables with plane seismic waves. *Geophysical Prospecting* 64: 671–88. doi:10.1111/1365-2478.12303.

Mateeva, A., J. Lopez, H. Potters, J. Mestayer, B. Cox, D. Kiyashchenko, P. Wills, et al. 2014. Distributed acoustic sensing for reservoir monitoring with vertical seismic profiling. *Geophysical Prospecting* 62: 679–92. doi:10.1111/1365-2478.12116.

Park, C., R. D. Miller, and J. Xia. 1999. Multichannel analysis of surface waves. *Geophysics* 64, no. 3: 800–8. doi: 10.1190/1.1444590

Parker, T., S. Shatalin, and M. Farhadiroushan. 2014. Distributed acoustic sensing – a new tool for seismic applications. *First Break* 32: 61–9. doi: 10.3997/1365-2397.2013034

Pevzner, R., K. Tertyshnikov, V. Shulakova, M. Urosevic, A. Kepic, B. Gurevich*, and R. Singh. 2015. Design and deployment of a buried geophone array for CO2 geosequestration monitoring: CO2CRC Otway Project, stage

2C. In *SEG technical program expanded abstracts 2015*, 266–70. SEG New Orleans Annual Meeting. doi:10.1190/segam2015-5902309.1.

Pevzner, R., M. Urosevic, E. Caspari, R. J. Galvin, M. Madadi, T. Dance, V. Shulakova, B. Gurevich, V. Tcheverda, and Y. Cinar. 2013. Feasibility of time-lapse seismic methodology for monitoring the injection of small quantities of CO2 into a saline formation, CO2CRC Otway Project. *Energy Procedia* 37: 4336–43. doi: 10.1016/j.egypro.2013.06.336

Pevzner, R., M. Urosevic, K. Tertyshnikov, B. Gurevich, V. Shulakova, S. Glubokovskikh, D. Popik, et al. 2017. Stage 2C of the CO2CRC Otway Project: seismic monitoring operations and preliminary results. *Energy Procedia*, in press.

Shulakova, V., R. Pevzner, J. C. Dupuis, M. Urosevic, K. Tertyshnikov, D. E. Lumley, and B. Gurevich. 2015. Burying receivers for improved time-lapse seismic repeatability: CO2CRC Otway field experiment. *Geophysical Prospecting* 63, no. 1: 55–69. doi: 10.1111/1365-2478.12174

White, D. 2011. Geophysical monitoring of the Weyburn CO2 flood: results during 10 years of injection. *Energy Procedia* 4: 3628–35. doi: 10.1016/j.egypro.2011.02.293

Yavuz, S., B. M. Freifeld, R. Pevzner, K. Tertyshnikov, A. Dzunic, S. Ziramov, V. Shulakova, et al. 2016. Subsurface imaging using buried DAS and geophone arrays – preliminary results from CO2CRC Otway Project. 78th EAGE Conference and Exhibition 2016, Th SBT4 04.